ADVANCED MATERIALS
www.advmat.de

Artificial Perspiration Membrane by Programmed Deformation of Thermoresponsive Hydrogels

*Junsoo Kim, Solyee Im, Jeong Hun Kim, Sang Moon Kim, Seung-Min Lee, Jaewoo Lee, Jong Pil Im, Jiyong Woo, and Seung Eon Moon**

Thermal management is essential for living organisms and electronic devices to survive and maintain their own functions. However, developing flexible cooling devices for flexible electronics or biological systems is challenging because conventional coolers are bulky and require rigid batteries. In nature, skins help to maintain a constant body temperature by dissipating heat through perspiration. Inspired by nature, an artificial perspiration membrane that automatically regulates evaporation depending on temperature using the programmed deformation of thermoresponsive hydrogels is presented. The thermoresponsive hydrogel is patterned into pinwheel shapes and supported by a polymeric rigid frame with stable adhesion using copolymerization. Both shape of the valve and mechanical constraint of the frame allow six times larger evaporation area in the open state compared to the closed state, and the transition occurs at a fast rate (≈1 s). A stretchable membrane is selectively coated to prevent unintended evaporation through the hydrogel while allowing swelling or shrinking of the hydrogel by securing path of water. Consequently, a 30% reduction in evaporation is observed at lower temperature, resulting in regulation of the skin temperature at the thermal model of human skins. This simple, small, and flexible cooler will be useful for maintaining temperature of flexible devices.

Biological and electronic systems require thermal management to maintain best performance because metabolism and electric current always generate heat and corresponding temperature change may degrade the performance.[1–5] Traditionally, the refrigeration cycle which employs compressors, condensers, and evaporators has been used to deal with most thermal issues. Thermoelectric coolers, which transport heat energy via electric carriers, have been also used for specific applications requiring simpler and smaller components.[6] However, cooling systems have generally been bulky and inflexible because the efficiency of the refrigeration cycle limits the size of the cooling device[7] and thermoelectric materials used in coolers are generally brittle and hard.[8,9] In addition to active components, complex auxiliary components such as power source, heat spreader, and heat sinks are also required. It generally prohibits their application to flexible electronics and biosystems.

By contrast, nature resolves the issues of heat management through perspiration.[10,11] Perspiration dissipates heat at the flexible skin surface by evaporating sweat through pores whose area is controlled by peripheral muscles. In principle, the energy density of perspiration is about 2 MJ kg^{-1} (latent heat of water),[12] which is high enough considering the cooling efficiency of traditional coolers and the energy density of batteries (≈2 MJ kg^{-1} in the case of lithium-ion batteries).[13]

Regulation of the evaporation rate is also important to prevent overcooling and wasting of sweat. The maximum evaporation rate is determined by environment condition such as humidity so cannot be controlled by the device. By contrast, it is possible to suppress evaporation on demand by blocking the evaporation area with valves like what peripheral muscles do for the perspiration. Therefore, the performance of evaporative cooler can be defined as the ability to control the evaporation area depending on the temperature. In microfluidic channels and biosystems, thermoresponsive hydrogels that swell and shrink in water depending on environmental temperature have been utilized to control pore size, which is potentially useful to mimic peripheral muscles regulating the evaporation depends on the temperature.[14–18] However, it is still challenging to use them for cooling, because the pore size of the hydrogels needs to be regulated at the water–air interface where evaporation happens. For instance, Park et al. recently introduced a smart membrane which was able to regulate pore size outside of the water, but it was unable to control the evaporation rate since it operated at saturated humidity.[19]

Here, we introduce an artificial perspiration membrane which automatically regulates evaporation rate at water–air

J. Kim,[+] S. Im, Dr. J. H. Kim, Dr. S.-M. Lee, Dr. J. Lee, Dr. J. P. Im, Dr. J. Woo, Dr. S. E. Moon
ICT Materials Research Group
Electronics and Telecommunications Research Institute
Daejeon 34129, Republic of Korea
E-mail: semoon@etri.re.kr
Prof. S. M. Kim
Department of Mechanical Engineering
Incheon National University
Incheon 22012, Republic of Korea
The ORCID identification number(s) for the author(s) of this article can be found under https://doi.org/10.1002/adma.201905901.
[+]Present address: John A. Paulson School of Engineering and Applied Science, Kavli Institute for Bionano Science and Technology, Harvard University, MA 02138, USA

DOI: 10.1002/adma.201905901

interface depending on temperature. This membrane consists of a valve structure and a rigid frame; the valve is made of silicone-coated thermoresponsive hydrogels and the frame is made of plastics. Those two components are stably bonded by copolymerization. By designing the shape of the valve and the mechanical constraint, we were able to control the area where evaporation occurs depending on temperature. As a result, the valves in the membrane open in a hot environment, which facilitates the evaporation of water, and the valves close in a cool environment, which suppresses the evaporation of water, mimicking cooling function of perspiration in a flexible manner. Our work shows the potential value of a bio-inspired, membrane-type, and automatic cooling device that can solve heat problems in artificial skin devices.

Figure 1 shows the components of the artificial perspiration membrane and its working principle. Our artificial perspiration membrane consists of two layers, a valve layer and a frame layer, which are made of poly(*N*-isopropylacrylamide) (PNIPAm) and polyurethane acrylate (PUA), respectively, and they are strongly bonded (Figure 1a). The low critical solution temperature, T_c, of PNIPAm is 32 °C,[20] which can also be engineered by using different materials, pH, or additives according to requirements of applications.[21–24] The diameter of a sweat gland is about 100 µm,[25] so we also used a similar size for the unit pattern which is arrayed on the membrane. While the valve structure swells and shrinks depending on temperature, the frame provides mechanical support to the mechanically weak valve structure and constrains the deformation of the valve at the edge.[26] Then, the assembled membrane covers the surface of water, where evaporation happens, so that the evaporation rate can be controlled according to dilation of the valve structure.

The evaporation area can be controlled by temperature change (Figure 1b). In the open operation, the valve shrinks and enlarges the area of water surface exposed to the air when the temperature is higher than T_c. In the close operation, the valve swells and covers the exposed water surface. The programmed deformation is key to this operation because the ratio of the area of valve and water basically cannot be changed by swelling as it is isotropic deformation. For example, if there is no mechanical constraint, the area of valve and the area of water surface will change with the same ratio, leading to the same evaporation per device area. Even if the valve is fixed at the boundary, straight rod or plane structures will be rather buckled toward out-of-plane direction so the area ratio still cannot be changed.[27,28] One possible way to convert swelling

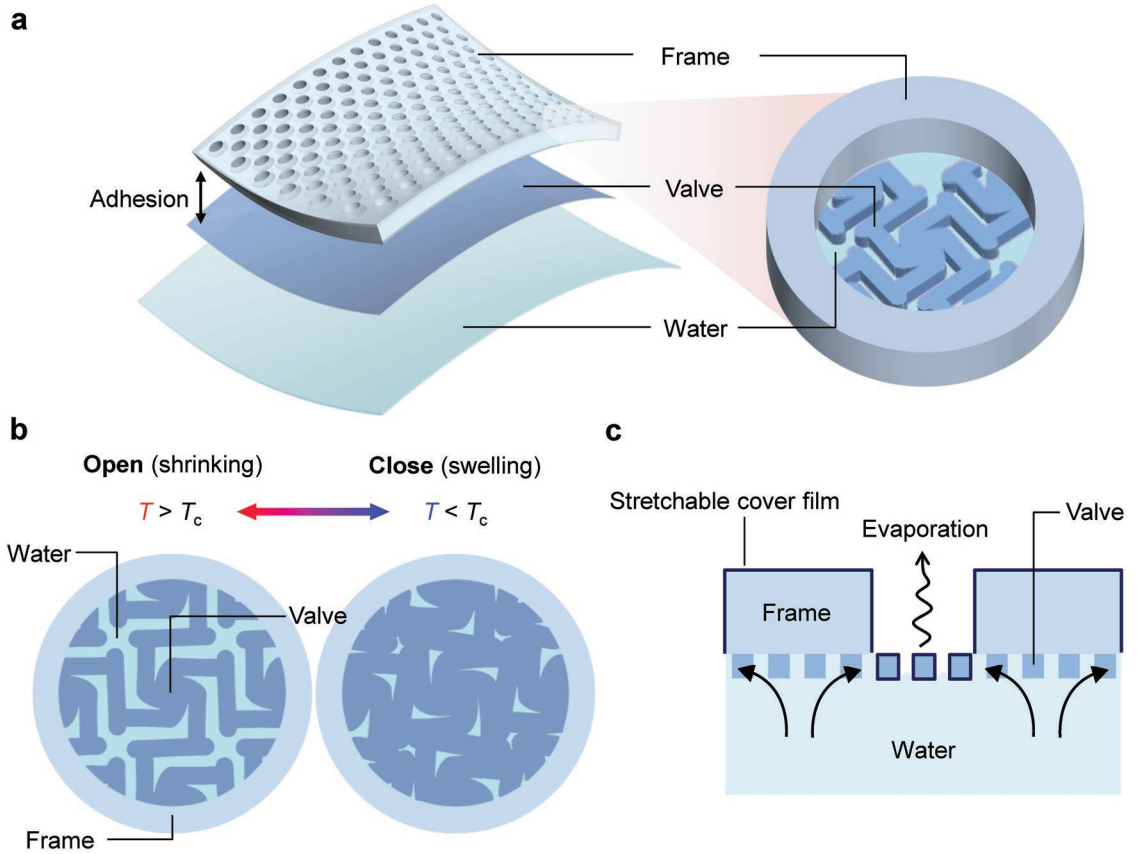

Figure 1. a) Schematic of artificial perspiration membrane. The membrane consists of a valve layer and a frame layer. The two membranes are bonded so the frame confines the deformation and supports the valve structure. Then, the membrane is floated on water and controls the evaporation area. b) Schematic of valve control mechanism. When the temperature is higher than a critical temperature, T_c, the valve structure shrinks and exposes the water to air. When the temperature is lower than T_c, the valve structure swells and covers the water surface. c) The valve structure is selectively coated by a stretchable cover film to prevent evaporation at the surface of the valve and to keep the water surface below the valve layer, but securing water path for swelling and shrinking.

into area change is to induce in-plane bending by adding a corner shape at the rod. As the volume increases, the stress will be concentrated around the corner and then induce in-plane bending before out-of-plane buckling occurs. In this study, we arrayed four rods containing a corner to form a symmetric unit pattern to cover whole area by simply repeating it, resulting in a pinwheel structure array. Finally, both the shape and the mechanical constraint of the valve will allow a distinctive deformation behavior for effective area change by the swelling.

The valve is covered by a nonswellable and stretchable film to prevent evaporation at the valve surface, and to keep the water surface below the valve (Figure 1c). We use a hydrophobic and relatively soft silicone rubber, Ecoflex 00–10, as the stretchable cover film. It is coated on the top side of the frame layer and the valve structures, blocking evaporation at the valve surface and preventing the valve from being immersed in the water. Since the valve beneath the frame is not coated by Ecoflex, the water can still reach the valve structure.

Our membrane is fabricated by assembling the valve layer and the frame layer based on a dewetting-based molding technique[29] (**Figure 2**a–e). Each layer is fabricated separately using a flat and a structured polydimethylsiloxane (PDMS) molds. The molds are fabricated using a conventional soft lithography procedure.[30] The precursor of each layer, PUA or PNIPAm, is poured onto each flat mold and squeezed with a structured mold until the two molds meet by dewetting process. After that, they are exposed to UV light for a limited time to get partially cured the membranes (Figure 2a–d). Because oxygen permeates through the PDMS, the surface of membrane is less cured compared to the core, so that we can handle the membrane with uncured precursors on the surface. The partially cured precursors have unreacted monomers and active radicals in the polymer chain, allowing additional polymerization after demolding. The proper UV exposure time for the PNIPAm was determined by quantifying the curing level over time based on the procedure conducted for PUA in previous studies[31] (Figure S1, Supporting Information). The partially cured PUA membrane is entirely peeled off from the molds and placed onto the partially cured PNIPAm sample after peeling only its flat mold off (Figure 2e). Note that the remaining structured PDMS mold of the PNIPAm structure is used as a substrate because the PNIPAm structure becomes crumpled if it is peeled off without a supporting layer. The unit pattern size of the valve is designed to be at least two times smaller than the diameter of the frame so that we do not have to align the two layers when they are assembled.[29] Then, we applied pressure and UV light to copolymerize the two materials at the interface, generating permanent adhesion.

Next, a stretchable cover film, Ecoflex, was selectively coated on the membrane to prevent evaporation at the valve surface

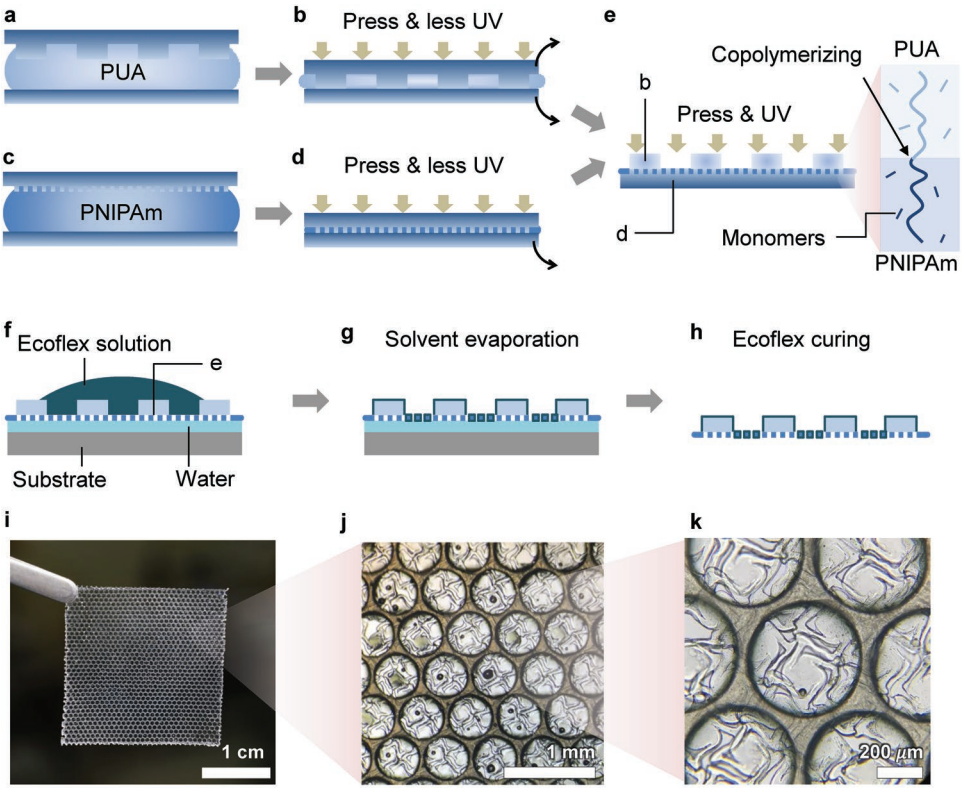

Figure 2. Fabrication of artificial perspiration membrane. a,b) Fabrication of frame layer. PUA precursor is poured between the PDMS mold and flat PDMS mold. UV light is exposed with pressure to produce a partially cured PUA frame layer. c,d) Fabrication of the valve layer. The partially cured PNIPAm layer is made the same way as the frame but the PDMS mold is not peeled off. e) The partially cured frame and valve are pressed and cured to induce copolymerizing at the interface. f–h) Ecoflex coating of the valve. The assembled layer is placed on the glass substrate with water, establishing a thin water layer to prevent the invasion of Ecoflex solution under the frame. The Ecoflex solution is poured onto the frame side and cured after evaporating its solvent. i–k) A fabricated artificial perspiration membrane photographed with a camera at different magnifications in the closed state. j–k) Optical microscope images are taken when the membrane absorbs cold water.

but to allow swelling and shrinking by securing a water path (Figure 2f–h). First, the membrane was placed onto a glass substrate with some water to induce conformal contact.[26] This interface is strong because of the high surface tension of the water, and prevents the Ecoflex solution from penetrating under the membrane. Then, the Ecoflex solution (diluted by hexane, 5 wt%) is poured on the membrane. Due to the difference in surface tension between hexane and water, the water–valve interface is not coated by Ecoflex. After evaporating the solvent, we cured the Ecoflex to obtain the final membrane. Detailed experimental setups of each step are displayed in Figure S2 of the Supporting Information.

The fabricated membrane is shown in Figure 2i–k at different magnifications. The membrane is self-supporting and the microsized valve structure remains stable with the aid of the attached frame. We confirmed the successful coating by observing the contact angles of water on the surfaces (Figure S3 and Movie S1, Supporting Information), the scanning electron microscope (SEM) images (Figure S4, Supporting Information), the energy-dispersive X-ray spectroscopy (EDS) (Figure S5, Supporting Information) of the membrane. The thickness of the coating was around 1 µm. Since the shear modulus of the Ecoflex and PNIPAm in our recipe have a similar order of magnitude ($\mu \approx 100$ kPa[32]) but the thickness of the coating is at least 1 order less than the valve, the Ecoflex film would merely affect the deformation. The replication fidelity was good enough to allow the valve deformation to be programed (Figure S6, Supporting Information).

The shape of the valve is key to changing the area of the water surface (**Figure 3**). To show how the valve design affects to the valve operations, we compared the deformation behaviors of two types of valve designs, a dot pattern which is simple pore array and a pinwheel pattern which is our design. To visualize the valve structure in 3D image, fluorescent dyes were grafted to the PNIPAm and scanned by confocal microscope. The structures of each design at two temperatures, 45 and 20 °C, are shown in Figure 3a–d. Top views and cross-section views are also presented bottom right of the perspective views and below the figure, respectively. In the case of the dot pattern (Figure 3a,b), symmetric expansion causes buckling. The cross-section view clearly shows the buckling of the valve, and the top view shows enlarged pores even though it is in the closed state. However, our design, the pinwheel structure, did not show buckling to the out of plane direction. Instead, the valve expanded along the plane and the pores are closed.

The deformation in each shape was compared by simulation using a commercial simulation tool, COMSOL. Details regarding the simulation are provided in Note S1 of the Supporting Information. The volume expansion ratio was measured from the confocal microscope images and then applied to the simulation to calculate the final shape and stress field. The simulation also showed that the dot pattern buckles,

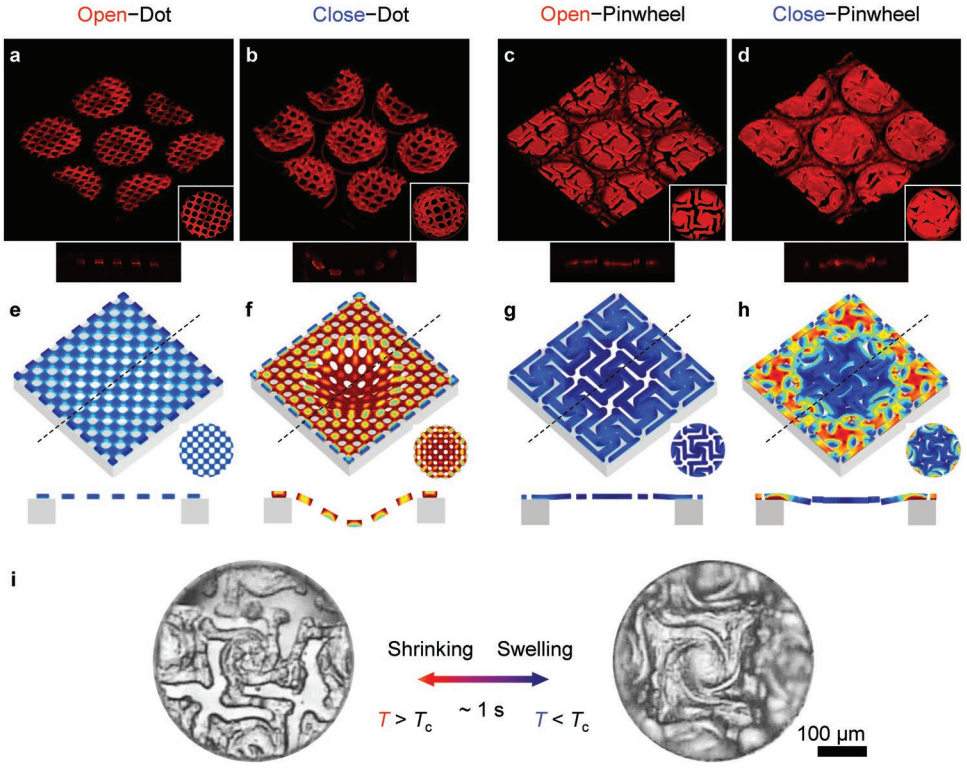

Figure 3. a–d) Confocal microscopy images and e–h) a simulation of the dot and pinwheel patterns in the opened and closed states. Top view and cross-section views are displayed in the inset and below the image, respectively. The dot pattern cannot close the valve (a,b and e,f) due to buckling, whereas the pinwheel pattern (c,d) opens and (g,h) closes the valve effectively. Simulations showing similar deformation shapes with experiments, and less residual stress in the pinwheel structure. The color scales of all images are identical. i) Optical microscope images of the valve structure at different temperatures. The membrane is floated onto the water surface. The valve is opened as the structure shrinks when the temperature is higher than T_c, and closed as the structure swells when the temperature is lower than T_c. The actuation time is on the order of 1 s.

and enlarges pores, with a lot of concentrated residual stress (Figure 3e,f). By contrast, the pinwheel structure successfully covered the exposed water area without buckling by effectively releasing the residual stress along the plane (Figure 3g,h).

Consequently, our design of the valve and mechanical constraint of the frame allowed efficient, repeatable, and fast valve operation at the water–air interface (Figure 3i; Movie S2, Supporting Information). When the temperature is higher than T_c, the valve structure is shrunk and exposed more water to the air. When the temperature is lower than T_c, the valve structure is swollen and covered more water with valve structure. The assembled layers maintained their shape even after multiple swelling and shrinking cycles (Figure S7, Supporting Information). From the top view, the area of exposed water surface in the open state is about six times larger than in the closed state (Figure S8, Supporting Information). The swelling and shrinking processes take about 1 s, respectively. Because the volume change is a diffusion process, the operating speed will be similar to the relaxation time of the valve structure.[33] Since the relaxation time τ is l^2/D, where D is the diffusivity of gels (10^{-10} m^2 s^{-1})[33] and l is the characteristic length (30 μm), the τ is expected to be 10 s, which is a reasonable value compared to the observation.

The artificial perspiration membrane is able to control the evaporation rate in relation to temperature (**Figure 4**). The evaporation rate, $\dot{m}$, the mass of evaporated water per area of membrane per time, was measured according to the temperature to quantify the performance of regulation.[34] A measurement setup was built to measure the loss of water through the membrane, under constant humidity and various temperatures (from 24 to 35 °C). We put the water and membrane on a balance and isolated those from the chamber, because any connection could cause a significant error when measuring the small amount of mass. Further discussion about the setup is provided in Figure S9 of the Supporting Information. Due to the temperature dependency of vapor pressure, the evaporation rate increases as temperature increases. Thus, we compared the artificial perspiration membrane and its reference, a valve made of PUA, to characterize its regulation performance.

The artificial perspiration membrane and the reference showed the same evaporation rate when the temperature was high because the valve shape in the open state was similar to the original mold shape (Figure 4a; Figure S6, Supporting Information). The evaporation rates became different when the temperature was less than 30 °C. To see the effect of valve operation, this difference in evaporation rate was normalized by the evaporation rate of the reference at each temperature (Figure 4b). The evaporation rate of the artificial perspiration membrane decreased as much as 30% compared to that of the reference sample. This value was lower than we expected from the area change of the membrane, because a six times difference in area is expected to induce an 84% evaporation rate difference. One possible reason of this is the vertical gaps of the pinwheel structure. Even though deformation is designed to happen along the plane, some parts of the pinwheel structure

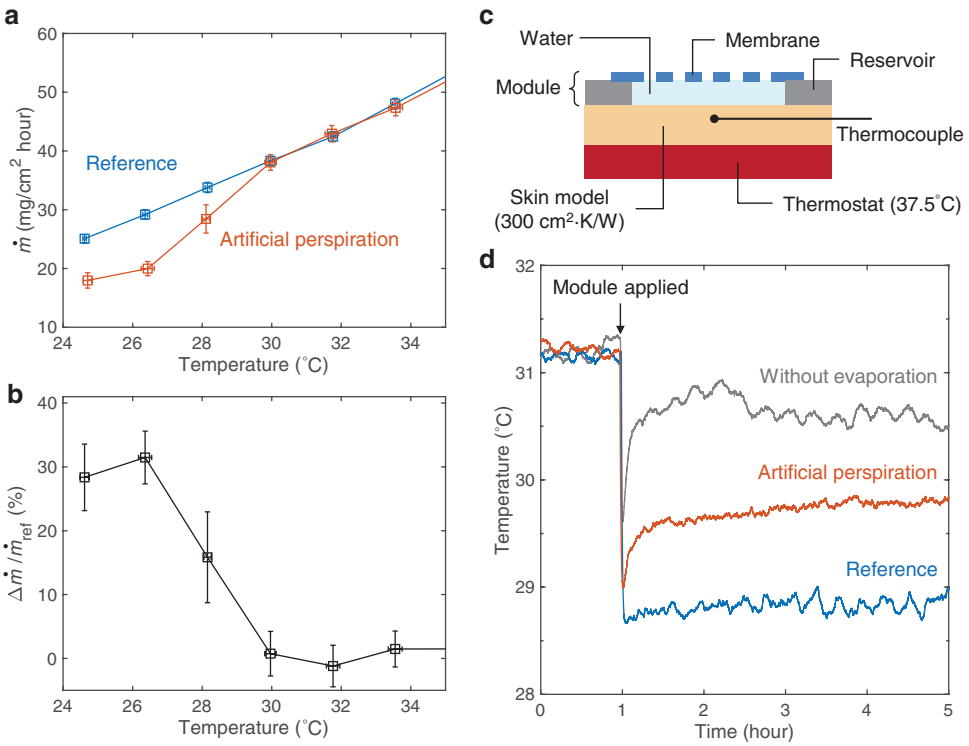

Figure 4. a) Evaporation rate measurement of reference and artificial perspiration membrane according to the temperature. b) Normalized evaporation rate difference according to temperature. The difference in evaporation rate increases when the temperature is less than 30 °C. c) Schematic of experiment setup of thermal model of human skins and the artificial perspiration module. d) Measured temperature of the skin model depending on three membranes; metal foil (without evaporation), reference, and our membrane. The skin model was cooled by evaporation and the temperature was regulated by our membrane.

are slightly tilted toward the out-of-plane direction, resulting in vertical gaps omitted in the area change calculation (Movie S3 and Figure S10, Supporting Information). Minimizing out-of-plane buckling will increase the performance of regulation.

Consequently, the regulation of cooling influenced to the temperature of a thermal model of human skins (Figure 4c,d; Figure S11, Supporting Information). We modeled human skins using a thermostat and a thermal insulator representing a blood and a skin, respectively (Figure 4c). The thermostat was fixed to be 37.5 °C and the thermal insulator was designed to have thermal resistance of 300 cm^2 K W^{-1} which is similar with human skins.[21] We placed the artificial perspiration module consisting of membrane, reservoir, and water, and then monitored the skin temperature. The three membranes; the metal foil, the reference, and the artificial perspiration membrane were tested on this skin model to demonstrate cooling and regulation performance (Figure 4d). The initial temperatures of all membranes were 31.2 °C. It is lower than the temperature of the thermostat because of the thermal resistance of the skin. The temperature was dropped to some extent when the module is placed, and then reached to equilibrium within 30 min. First, we blocked evaporation with metal foils to see other cooling effects such as heat transfer. The equilibrium temperature dropped 0.7 °C. Second, in the case of the reference which evaporates water without regulation, the equilibrium temperature dropped 2.2 °C because the evaporation dissipates heat in addition to the heat transfer. The PNIPAm structure without Ecoflex coating gives similar results (Figure S11, Supporting Information). In the case of the artificial perspiration membrane, however, the temperature dropped only 1.4 °C since the evaporation area was reduced as it is in the closed state. These results show that evaporation can cool human skins down and our membrane can regulate its cooling power. Also, this regulation performance was durable (Figure S11, Supporting Information).

We introduce an artificial perspiration membrane that regulates the evaporation area based on temperature. The membrane consists of a valve layer made of PNIPAm and its frame layer made of PUA with a selective coating of Ecoflex. We attached the PNIPAm layer and the PUA layer stably by copolymerizing two surfaces, so that the frame supports the weak valve structure and confines the deformation to permit opening and closing functions. The deformation of the valve structure was analyzed with 3D images of a confocal microscope. The pinwheel shape of the valve allows effective deformation for opening and closing operations by preventing out-of-plane buckling. The valve operation is fast enough as the structure is microsized and is repeatable. As the valve opens and closes the pores depending on the temperature, the evaporation rate was changed. Finally, we showed that the skin temperature of the thermal model of human skins can be regulated by our membrane. Our study on a smart membrane that can automatically regulate cooling power without external power source may solve thermal problems in wearable or artificial skin devices.

Experimental Section

Fabrication of Artificial Perspiration System: The frame and the valve structure pattern were fabricated from PDMS mold fabricated using a conventional soft lithography technique. Commercial PUA-based UV-curable precursor, MINS-301 (Minuta tech, Korea), was drop casted between a PDMS mold and a flat PDMS mold. UV light (λ = 250–400 nm, intensity ≈1.5 mW cm^{-2}) was exposed for about 1 min with pressure (≈60 kPa) to partially cure the structure. After peeling off the PDMS mold, the film was temporarily stored on the PDMS surface. To synthesize the thermoresponsive hydrogel, *N*-Isopropylacrylamide, *N*,*N*′-Methylenebisacrylamide, dimethyl sulfoxide, deionized water, and 2-hydroxy-2-methylpropiophenone were mixed at a weight ratio of 2.18:0.12:3:1:0.2 and stirred overnight at room temperature. The mixture was drop casted onto the PDMS valve mold and sandwiched with the flat PDMS mold, and then exposed to UV for about 2 min with pressure (≈60 kPa) resulting in a partially cured valve structure. Then, just the flat mold was removed and the partially cured frame was placed on the valve structure. UV exposure with pressure (≈10 kPa) was applied for more than 10 min to fully cure the interface. The final structure was rinsed with DI water.

Characterizations of Ecoflex Coating: The commercial contact angle equipment (Smartdrop, Femtobiomed) was used to measure the contact angles. A focused ion beam (FIB, Helios Nanolab 450 F1) was used for scanning of the cross-sectional images. Ga ion beam was exposed to dissect the valve structures. Elemental characterization was carried out by EDS attached to the FIB instrument.

3D Imaging of Artificial Perspiration System: The procedure described in the reference paper was followed to graft Rhodamin B fluorescent dye onto the PNIPAm chain.[35] A membrane fabricated with the dyed PNIPAm precursor was laid on the plate with a hole to float the valve structure above the floor. The membrane was scanned by confocal microscope (LSM510-Meta NLO, Carl Zeiss).

Evaporation Measurement: The mass of the water was measured using a balance and the data were logged by computer in real time. The evaporation rate was calculated from the slope at the mass–time plot. Details are in the Supporting Information.

Temperature Measurement with the Thermal Model of Human Skins: The thermostat is made of a copper block. Heaters and thermocouple are embedded in the block and the temperature was controlled using the PID controller (Lakeshore 335). The thermal insulator of 6 mm thick Ecoflex block (thermal conductivity ≈0.2 W m^{-1} K^{-1})[36] made by molding was put onto the thermostat. The temperature of the skin model was measured at 2 mm below from the top using thermocouple. The modules are applied after the skin model was in equilibrium with environment which is natural convection of 22 °C air.

Supporting Information

Supporting Information is available from the Wiley Online Library or from the author.

Acknowledgements

This work was supported by the National Research Council of Science & Technology (NST) grant by the Korea government (MSIP) (No. CAP-14-01-KIST), by the Materials and Components Technology Development Program of MOTIE/KEIT, Republic of Korea (No. 10063286, Development of high efficient thermoelectric module with figure of merit (Z) 3.4(×10^{-3}) by using 1.0 kg per batch scale producible polycrystalline thermoelectric material with average figure of merit (*ZT*) 1.4 and over"), and by Electronics and Telecommunications Research Institute (ETRI) grant funded by the Korean government (19ZB1800).

Conflict of Interest

The authors declare no conflict of interest.

Keywords

artificial perspiration, programmed deformation, smart membranes, thermoresponsive hydrogels

Received: September 9, 2019
Revised: October 16, 2019
Published online:

[1] R. Ma, Z. Zhang, K. Tong, D. Huber, R. Kornbluh, Y. S. Ju, Q. Pei, *Science* **2017**, *357*, 1130.
[2] S. Bauer, *Nat. Mater.* **2013**, *12*, 871.
[3] N. N. Shi, C.-C. Tsai, F. Camino, G. D. Bernard, N. Yu, R. Wehner, *Science* **2015**, *349*, 298.
[4] X. A. Zhang, S. Yu, B. Xu, M. Li, Z. Peng, Y. Wang, S. Deng, X. Wu, Z. Wu, M. Ouyang, Y. Wang, *Science* **2019**, *363*, 619.
[5] Y. Chen, B. Lu, Y. Chen, X. Feng, *Sci. Rep.* **2015**, *5*, 11505.
[6] S. Twaha, J. Zhu, Y. Yan, B. Li, *Renewable Sustainable Energy Rev.* **2016**, *65*, 698.
[7] S. Jeong, *Int. J. Refrig.* **2004**, *27*, 309.
[8] J. He, T. M. Tritt, *Science* **2017**, *357*, eaak9997.
[9] S. Il Kim, K. H. Lee, H. A. Mun, H. S. Kim, S. W. Hwang, J. W. Roh, D. J. Yang, W. H. Shin, X. S. Li, Y. H. Lee, G. J. Snyder, S. W. Kim, *Science* **2015**, *348*, 109.
[10] P. Tao, W. Shang, C. Song, Q. Shen, F. Zhang, Z. Luo, N. Yi, D. Zhang, T. Deng, *Adv. Mater.* **2015**, *27*, 428.
[11] T. Kokalj, H. Cho, M. Jenko, L. P. Lee, *Appl. Phys. Lett.* **2010**, *96*, 163703.
[12] B. H. Sellers, *Q. J. R. Meteorol. Soc.* **1984**, *110*, 1186.
[13] J. M. Tarascon, M. Armand, *Nature* **2001**, *414*, 359.
[14] D. J. Beebe, J. S. Moore, J. M. Bauer, Q. Yu, R. H. Liu, C. Devadoss, B.-H. Jo, *Nature* **2000**, *404*, 588.
[15] S. Cui, Y. Hu, Z. Huang, C. Ma, L. Yu, X. Hu, *Int. J. Therm. Sci.* **2014**, *79*, 276.
[16] Z. Huang, X. Zhang, M. Zhou, X. Xu, X. Zhang, X. Hu, *J. Electron. Packag.* **2012**, *134*, 31.
[17] Z. Liu, W. Wang, R. Xie, X.-J. Ju, L.-Y. Chu, *Chem. Soc. Rev.* **2016**, *45*, 460.
[18] X. Hou, *Adv. Mater.* **2016**, *28*, 7049.
[19] Y. Park, M. P. Gutierrez, L. P. Lee, *Sci. Rep.* **2016**, *6*, 2793.
[20] D. H. Kang, S. M. Kim, B. Lee, H. Yoon, K.-Y. Suh, *Analyst* **2013**, *138*, 6230.
[21] V. Leonov, *IEEE Sens. J.* **2013**, *13*, 2284.
[22] Q. Li, C. Gao, S. Li, F. Huo, W. Zhang, *Polym. Chem.* **2014**, *5*, 2961.
[23] X. Lu, A. Z. Hu, J. Schwartz, *Macromolecules* **2002**, *35*, 9164.
[24] L. Starovoytova, J. Šťastná, A. Šturcová, R. Konefal, J. Dybal, N. Velychkivska, M. Radecki, L. Hanyková, *Polymers* **2015**, *7*, 2572.
[25] K. Wilke, A. Martin, L. Terstegen, S. S. Biel, *Int. J. Cosmet. Sci.* **2007**, *29*, 169.
[26] J. Kim, Y. Wang, H. Park, M. C. Park, S. E. Moon, S. M. Hong, C. M. Koo, K.-Y. Suh, S. Yang, H. Cho, *Adv. Mater.* **2017**, *29*, 1605078.
[27] S. Xu, Z. Yan, K.-I. Jang, W. Huang, H. Fu, J. Kim, Z. Wei, M. Flavin, J. McCracken, R. Wang, A. Badea, Y. Liu, D. Xiao, G. Zhou, J. Lee, H. U. Chung, H. Cheng, W. Ren, A. Banks, X. Li, U. Paik, R. G. Nuzzo, Y. Huang, Y. Zhang, J. A. Rogers, *Science* **2015**, *347*, 154.
[28] Y. Ma, K.-I. Jang, L. Wang, H. N. Jung, J. W. Kwak, Y. Xue, H. Chen, Y. Yang, D. Shi, X. Feng, J. A. Rogers, Y. Huang, *Adv. Funct. Mater.* **2016**, *26*, 5345.
[29] H. Cho, J. Kim, H. Park, J. W. Bang, M. S. Hyun, Y. Bae, L. Ha, D. Y. Kim, S. M. Kang, T. J. Park, S. Seo, M. Choi, K.-Y. Suh, *Nat. Commun.* **2014**, *5*, 3137.
[30] D. Qin, Y. Xia, G. M. Whitesides, *Nat. Protoc.* **2010**, *5*, 491.
[31] H. Cho, S. M. Kim, Y. S. Kang, J. Kim, S. Jang, M. Kim, H. Park, J. W. Bang, S. Seo, K.-Y. Suh, Y.-E. Sung, M. Choi, *Nat. Commun.* **2015**, *6*, 8484.
[32] T. R. Matzelle, G. Geuskens, N. Kruse, *Macromolecules* **2003**, *36*, 2926.
[33] Z. I. Kalcioglu, R. Mahmoodian, Y. Hu, Z. Suo, K. J. Van Vliet, *Soft Matter* **2012**, *8*, 3393.
[34] Z. Wang, Y. Liu, P. Tao, Q. Shen, N. Yi, F. Zhang, Q. Liu, C. Song, D. Zhang, W. Shang, T. Deng, *Small* **2014**, *10*, 3234.
[35] J. Kim, J. A. Hanna, M. Byun, C. D. Santangelo, R. C. Hayward, *Science* **2012**, *335*, 1201.
[36] M. D. Bartlett, N. Kazem, M. J. Powell-Palm, X. Huang, W. Sun, J. A. Malen, C. Majidi, *Proc. Natl. Acad. Sci. USA* **2017**, *114*, 2143.

